Rayleigh wave phase velocities and upper mantle structure in the Apennines *

M. Caputo (¹) – L. Knopoff (²) –
E. Mantovani (³) – St. Mueller (⁴) – G. F. Panza (⁵) (**)

Received on September 26th, 1976

Summary. — The dispersion of the phase velocities of the surface Rayleigh waves on the path between the station pair Torino-L'Aquila in the Apennines has been observed with long period seismic stations for twin earthquakes.

The inversion was provided by the "Hedgehog" program of non-linear inversion analysis.

The interpretation supports the notion that in the Apennines low-velocity material in the mantle is found within a few km of the Moho and may lie immediately below the Moho; however the alternative model of a high-velocity lid and very low-velocity channel cannot be completely rejected.

Riassunto. — Mediante stazioni sismiche a lungo periodo, è stata studiata, per terremoti gemelli, la dispersione della velocità di fase delle onde superficiali tipo Rayleigh. in un tragitto compreso fra le stazioni di Torino e L'Aquila, lungo gli Appennini.

L'inversione è stata fornita dal programma "Hedgehog" per l'analisi d'inversione non-lineare.

(*) Publication Nr. 1570, Institute of Geophysics and Planetary Physics, University of California – Los Angeles.

Mitteilung Nr. 141, Institut für Geophysik – ETH Zürich.

(1) Istituto di Geofisica, Roma – Università di Bologna.

(2) Institute of Geophysics & Planetary Physics, University of California – Los Angeles.

(3) Osservatorio Geofisico – Università di Siena.

(4) Institut für Geophysik Eidgenösische Technische Hochschule – Zürich.

(5) Istituto di Geodesia e Geofisica – Università di Bari, and Dipartimento di Scienze della Terra, Università degli Studi – Cosenza.

(**) Authors listed in alphabetical order.

L'interpretazione suggerisce che, in corrispondenza degli Appennini, materiale a bassa velocità si trovi nel mantello in una zona compresa fra pochi km sopra la Moho e immediatamente sotto, non escludendo completamente, tuttavia, il modello alternativo di una coltre ad alta velocità e di un canale a velocità molto bassa.

Introduction

The development of techniques for inversion of Rayleigh wave dispersion data has been a significant factor in delineating lateral inhomogeneities in the earth's crust and upper mantle. The pioneering activities in the measurement of dispersion were carried out by Brune and Dorman (1963) (7) for the Canadian Shield and by Knopoff et al. (1966) (14) for the Alps. Since that time, a considerable quantity of data has been amassed regarding Rayleigh wave dispersion in many parts of the world.

However, the systematic interpretation of these observations was not possible until the geophysical inverse problem was developed into a practical and efficient tool. Inversion studies have been carried out on two fronts. First, the linear inverse problem has been studied from the point of view of eigenvalue-eigenfunction analysis of non-square matrices for underdetermined systems of equations; these matrices characterize the problems of determining real earth structure from insufficient amounts of data (Backus and Gilbert, 1968, (1) 1970; (2) Jackson, 1972) (11). Second, the non-linear inverse problem has been attacked by a systematic attempt to construct the space of parameterized models, consistent, with the observations within certain error bounds (Biswas and Knopoff, 1974; (4) Knopoff and Schlue, 1972) (15).

The application of these techniques to the study of relatively stable parts of the earth has led to some important generalizations regarding the structure of the upper mantle:

1. – Under all the ancient preCambrian shields of the world, no significant low-velocity channel exists (Knopoff, 1972). (13) These parts of the continents have a root which extends to great depths. The absence of a well-developed low-velocity channel implies temperatures well below the melting point of mantle rocks; this is associated with *sub-normal* surface heat flow, and hence with geotherms which do not intersect the solidus.

2. – Under all the younger stable continental regions of the world, a well-developed low-velocity channel exists starting at a depth

of about 90 km (Knopoff, 1972) [13]. The shear-wave velocity contrast between lid and channel is about 0.3 km/sec. These values of shear velocity in the channel imply temperatures above the solidus and hence partial melting of the mantle rocks in this region; this is associated with *normal* surface heat flow, and hence with geotherms which intersect the solidus.

3. – Under the Pacific, a well-developed low-velocity channel exists, with a shear-wave velocity contrast between lid and channel of about 0.5 km/sec. The thickness of the lid increases with increasing lithospheric age (Leeds et al., 1974) [17], starting with zero thickness at the East Pacific Rise and increasing to about 100 to 110 km at a lithospheric age of 150 my (Leeds, 1975) [16]. The interface between lid and channel appears to be at the solidus for a wet peridotite.

Although the mantle under the stable parts of the world appear to have systematically similar properties, the less stable parts have been less thoroughly studied. Notable among these less stable areas are the mountainous regions of the world. Although some of the world's mountainous regions have been explored using surface waves, the mantle under these regions have not as yet shown any major tendency toward systematization. Among the individual areas studied, we can list regions associated with subduction zones (James, 1971) [12], rift zones (Biswas and Knopoff, 1974 [4]; Knopoff and Schlue, 1972 [15]; Seidl et al., 1970) [20] and folded belts (Knopoff, et al., 1966) [14].

It is reasonably easy to see why mountainous regions are difficult to understand. They are the surface expression of major tectonic activity either in the present or in the past. Thus, in some complex way, they reflect extraordinary stress conditions, such as those found at plate margins. The several types of tectonic interaction may have correspondingly different types of mantle structure beneath their respective surface expressions. By studying the upper mantle structure underneath mountainous regions, we have the possibility of learning something about the depth range of interaction stresses at plate boundaries and possibly something about the thermal regime in these areas.

One of the most accessible areas for this kind of study is the Italian peninsula. Italy may be an artifact of an earlier episode of tectonic activity in which the Alps were formed, and in which the Western Basin of the Mediterranean was opened up, perhaps contemporaneously with the rotation of the Iberian Peninsula. In any case, the upper mantle under the Western Basin seems to have a more or less *normal* oceanic structure at depth, with a possible transition structure at the top of the lid (Berry and Knopoff, 1967) (3); the Alps have an extraordinarily well-developed channel at relatively shallow depths, with the lowest channel *S*-wave velocity reported for any continental region, except for the East African Rift (Knopoff et al., 1966) (14); the islands of Sardinia and Corsica have no significant seismicity and may have *normal* upper mantle structure for young stable continental regions (Berry and Knopoff, 1967) (3). There is volcanism in the southern part of Italy, earthquakes abound in the entire peninsula and especially to the south of the Po Valley, there is geothermal activity over the entire peninsula, and deep-focus earthquakes and high heat flows are found in the Tyrrhenian Sea. Evidently Italy is surrounded by regions with widely different tectonic settings and with widely different crust and mantle structures; these structures are changing rapidly with lateral distance. For these reasons, it is of especial interest to try to determine the upper mantle structure beneath the Italian Peninsula, and perhaps to determine the tectonic processes that could give rise to this structure. In this paper, we report on a first step in this program.

Data

In a cooperative program originated by the Institut für Geophysik, Swiss Federal Institute of Technology, Zurich, the Institute of Geophysics, University of California, Los Angeles and the Istituto di Geofisica, University of Bologna, a network of long-period seismic stations has been installed over the entire length of the Italian Peninsula. Each station is equipped with 15-100 Sprengnether (WWSSN equivalent) seismographs. All of the stations have a vertical-component seismograph and some are equipped with three components. The stations are:

OLB	Olbia
TNO	Torino
BLZ	Bolzano
BOL	Bologna
BAR	Bari
NPL	Napoli
PLM	Palermo
CAG	Cagliari
GRO	Grosseto
ROM	Roma

These stations are used to supplement the existing WWSSN stations

AQU L'Aquila

TRI Trieste

to form a relatively dense network. The first of these stations was installed in 1970; all have been operating for varying lengths of time since their installation.

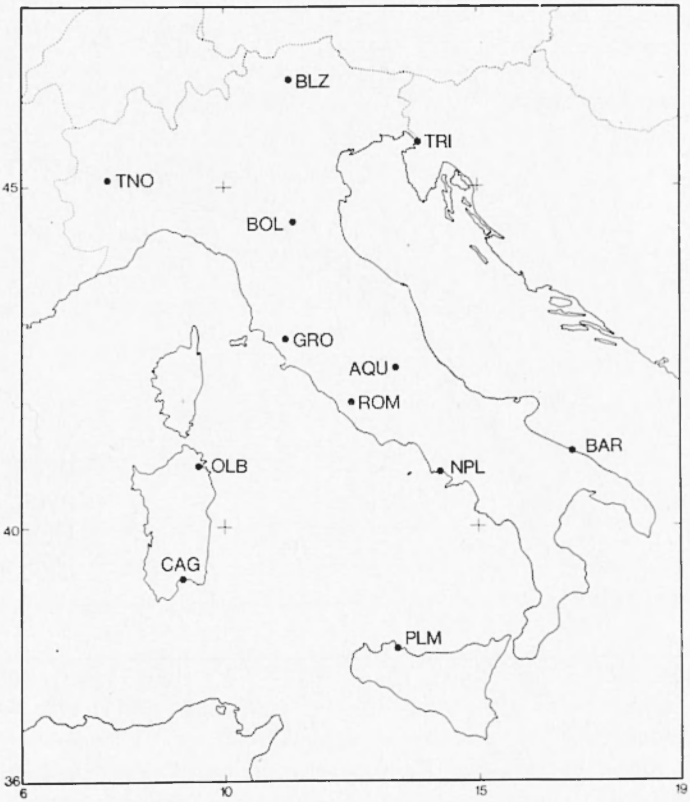

Fig. 1 – Map of Italian Peninsula showing network of long-period seismographs.

In this paper, we report on the result of processing seismograms taken for twin earthquakes in the North Atlantic at 54.3°N, 35.1°W:

Event 1: 3 April 1972 18:52:59.3 $M_s = 5.7$

Event 2: 3 April 1972 20:36:22.2 $M_s = 5.5$

The two events give different phase velocities because of the different signal-to-noise ratios and the varying character of the noise; errors in the analysis due to regional refractions of the surface waves outside the station pair cannot be assessed in this analysis; however, studies of surface waves in the Alps emanating from events in this part of the Atlantic showed few if any refraction effects (Knopoff, et al., 1966 ([14]).

The records for the station pair TNO and AQU were analyzed by time-windowing and frequency-filtering techniques described by

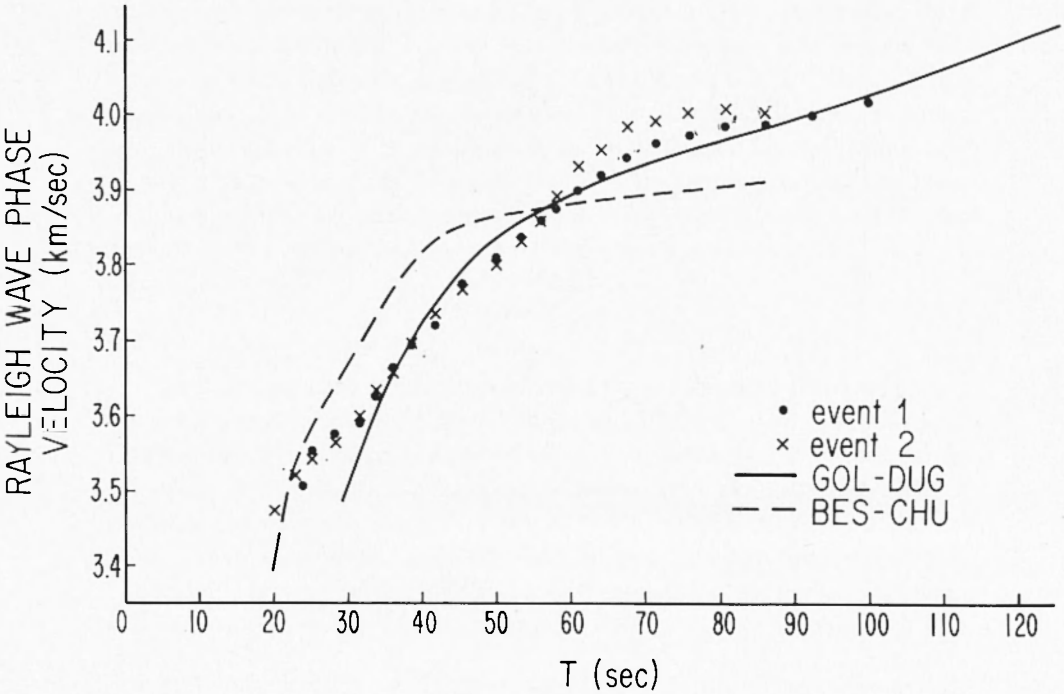

Fig. 2 – Measured Rayleigh wave phase velocities for events 1 and 2 for path TNO-AQU. Comparison can be made with measured phase velocities for Alpine path BES-CHU and U.S. path GOL-DUG.

Pilant and Knopoff (1964) ([19]) and Knopoff et al. (1966) ([14]) and refined by Biswas and Knopoff (1974) ([4]), Panza (1976) ([18]). The nominal great circle paths to the stations from these earthquakes are within 3° of the station pair line. The results of the phase velocity analyses are given in Table 1 for selected values of the multiples of the folding

TABLE I
Path TNO-AQU – Phase velocities (km/sec)

T (sec)	c_1	c_2	$\bar{c}$	c_f
100.0	4.012		4.012	3.949
92.6	3.997			
86.2	3.983	4.001		
80.7	3.981	4.005	3.993	3.942
75.8	3.969	4.000		
71.4	3.958	3.991		
67.6	3.936	3.983		
64.1	3.916	3.952		
61.0	3.896	3.931	3.914	3.875
58.1	3.873	3.889		
55.6	3.859	3.858		
53.2	3.835	3.830		
50.0	3.809	3.799	3.804	3.774
45.5	3.771	3.767		
41.7	3.719	3.735	3.727	3.702
38.5	3.693	3.696		
35.7	3.664	3.657		
33.3	3.624	3.632		
31.3	3.591	3.598	3.594	3.577
27.8	3.576	3.565		
25.0	3.555	3.539	3.547	3.533
23.8	3.506			
22.7		3.521	3.521	3.509
20.8		3.472		
20.0		3.474		

frequency; the values are listed as c^1 and c^2 for the two earthquakes. Although the values of c are listed to three decimals, this is merely a literal interpretation of the computer output; the results are accurate only to several hundredths of a km/sec. The maximum phase velocity differences between c^1 and c^2 are 0.04 km/sec, which may easily arise due to the small station pair distance interval.

INVERSION

For the purposes of inversion, a data set $\bar{c}$ was created which is a simple average of the values where available. These *spherical-earth* Rayleigh-wave phase-velocity values were reduced by the Bolt-Dorman

TABLE II

Cross section used in the inversion

Depth (Km)		Layer Thickness (km)	S-Wave Velocity (km/sec)	P-Wave Velocity (km/sec)	Density (gm/cm³)
0					
	CRUST	P1	3.7	6.4	3.00
Moho					
	LID	P2	P4	8.0	3.43
	CHANNEL	P3	P5	7.8	3.45
	SUBCHANNEL	$295-\sum_{N=1}^{3} P_N$	4.52	8.3	3.50
295					
	SUBCHANNEL	106	4.6	8.5	3.55
401					
		∞	5.0	9.15	3.75

confidence limits $\sigma = 0.03$ km/sec

single point rejection if $|\Delta c| > 0.05$ km/sec

parameter	range	starting value
P1	35(10)65	55
P2	20(10)60	40
P3	10(20)150	50
P4	4.21(0.1)4.61	4.31
P5	4.13(0.1)4.53	4.23

provided by the *Hedgehog* program of non-linear inversion analysis. The cross-section used in the inversion is listed in Table II. Our structure consists simply of five layers overlying a half-space, the latter beginning at a fixed depth of 401 km. The crust has no velocity gradient associated with it. The subchannel begins where the channel terminates, but in any case it begins at a depth of less than 295 km.

The subchannel is divided into two regions with a small velocity difference between them; the lower portion has a fixed thickness of 106 km. The *P*-wave velocities and densities of the layers are fixed; numerical experimentation has shown that the values of these two parameters can differ from those used by substantial amounts, e.g., 0.5 km/sec for *P*-wave velocity and 0.3 gm/cm³ for density, without significantly altering the phase velocities in this period range; this is another way of stating that fundamental mode Rayleigh wave phase velocities in this period range depend almost completely on the shear wave structure of the upper mantle.

There are five parameters in the Hedgehog search, namely the crustal, lid and channel thicknesses and the lid and channel *S*-wave velocities. These parameters are identified as P1 to P5 in Table II. The search takes place in the space of grid variables x_n, $n = 1,2,3,4,5$, where

(crustal thickness)	P1	$= 35 < 55 + 10x_1 \leqslant 65$ km
(lid thickness)	P2	$= 20 \leqslant 40 + 10x_2 \leqslant 60$ km
(channel thickness)	P3	$= 10 \leqslant 50 + 20x_3 \leqslant 150$ km
(lid velocity)	P4	$= 4.21 \leqslant 4.31 + 0.1x_4 \leqslant 4.61$ km/sec
(channel velocity)	P5	$= 4.13 \leqslant 4.23 + 0.1x_5 \leqslant 4.53$ km/sec

i.e., the allowable values of x_n are

$$x_1 = -2, -1, 0, 1$$
$$x_2 = -2, -1, 0, 1, 2$$
$$x_3 = -2, -1, 0, 1, 2, 3, 4, 5$$
$$x_4 = -1, 0, 1, 2, 3$$
$$x_5 = -1, 0, 1, 2, 3$$

with the point (0,0,0,0,0) as the starting point in the search. All solutions in the singly connected space $\{x_n\}$ are acceptable if the value of phase velocity predicted by the model differs from values listed as c_f in Table I by less than 0.05 km/sec at each of the eight periods and the root-mean-square of all eight differences is less than 0.03 km/sec. These estimates of error are based on past experience in processing seismograms of the quality of those obtained for these two events, the spacing between the stations and the similarity of the results for the two events.

The result of the Hedgehog inversion is presented in Table III; values of $\{x_n\}$ are listed as well as the values of the *rms* deviation between the model curve and the observations over the eight selected

Table III

Successful Solutions

Solution Number	$\{x_n\}$					σ	Solution Number	$\{x_n\}$					σ
1	0	0	0	0	0		40	0	−1	3	1	1	.027
2	0	1	0	0	0	.029	41	0	1	3	1	1	.028
3	0	0	1	1	0	.026	42	0	0	3	0	1	.027
4	0	0	0	1	−1	.027	43	0	−1	3	0	1	.026
5	−1	0	0	−1	−1	.029	44	0	1	3	0	1	.027
6	0	−1	1	1	0	.026	45	0	−2	3	1	1	.027
7	0	1	1	1	0	.026	46	0	−2	3	0	1	.027
8	0	1	1	0	1	.028	47	0	−2	3	2	1	.030
9	0	−1	0	1	−1	.028	48	0	2	3	1	1	.029
10	0	1	0	1	−1	.026	49	0	2	3	0	1	.028
11	0	2	0	0	0	.029	50	0	−1	1	3	−1	.028
12	0	2	0	1	0	.030	51	0	−2	2	3	0	.026
13	0	2	1	1	0	.027	52	0	−2	3	3	0	.029
14	0	2	−1	0	−1	.029	53	0	−2	3	−1	1	.030
15	0	2	1	0	1	.027	54	0	0	4	1	1	.027
16	0	2	0	1	−1	.027	55	0	−1	4	1	1	.026
17	0	0	2	1	0	.028	56	0	1	4	1	1	.028
18	0	−1	2	1	0	.028	57	0	0	4	0	1	.027
19	0	1	2	1	0	.028	58	0	−1	4	0	1	.027
20	0	−1	1	2	0	.028	59	0	1	4	0	1	.028
21	0	0	2	2	0	.030	60	0	−2	4	2	1	.028
22	0	0	2	1	1	.030	61	0	−2	4	1	1	.026
23	0	0	1	2	−1	.029	62	0	−2	4	0	1	.026
24	0	−1	2	2	0	.027	63	0	2	4	1	1	.028
25	0	−1	2	1	1	.030	64	0	2	4	0	1	.029
26	0	1	2	1	1	.030	65	0	2	4	0	2	.028
27	0	0	0	2	−1	.029	66	0	0	5	1	1	.027
28	0	0	2	0	1	.027	67	0	−1	5	1	1	.026
29	0	−1	0	2	−1	.027	68	0	1	5	1	1	.028
30	0	−1	2	0	1	.027	69	0	0	5	0	1	.028
31	0	1	2	0	1	.027	70	0	−1	5	0	1	.027
32	0	−2	1	1	0	.027	71	0	1	5	0	1	.029
33	0	−2	2	1	0	.029	72	0	1	5	0	2	.029
34	0	−2	1	2	0	.026	73	0	−2	5	1	1	.025
35	0	−2	2	2	0	.026	74	0	−2	5	0	1	.027
36	0	2	2	1	0	.028	75	0	−2	5	2	1	.027
37	0	2	2	0	1	.027	76	0	2	5	1	1	.028
38	0	0	3	1	1	.028	77	0	2	5	0	1	.030
39	0	−1	3	2	0	.030	78	0	2	5	0	2	.027

periods. Seventy-eight successful solutions were obtained. These solutions are plotted in a four-dimensional representation of the space $\{x_n\}$ in Fig. 3.

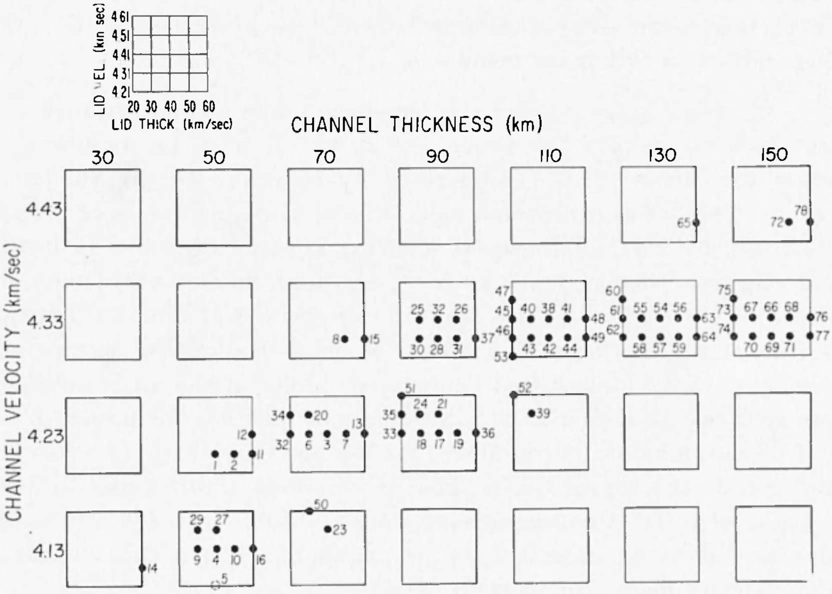

Fig. 3 – Four-dimensional space of acceptable solutions obtained from Hedgehog inversion.

Interpretation

1. All solutions except one (No. 5) have a crustal thickness of 55 km ($x_1 = 0$). All other crustal thicknesses are rejected. We believe that this severe restraint on x_1 is a consequence of the simplistic model of the crust that we have assumed. If we had used a crust with a velocity gradient, especially with lower velocities at the top of the crust, we would have obtained a somewhat thinner crust. However, the value we have obtained is related in some measure to the vertical travel time of S-waves through the crust; since the crustal S-wave velocities cannot be altered by more than several tenths of a km/sec, the thickness will not be reduced by much more than about 10 km or so. (In Fig. 3, all solutions are plotted as solid circles, except No. 5, which has a different crustal thickness and is shown dotted). Because of the *apparent* resolution of the crustal thickness, we have used only the

four remaining parameters in the diagram of acceptable solutions in Fig. 3.

The case of solution No. 5, with its decreased crustal thickness, requires much lower mantle velocities than the other solutions to keep the vertical travel time in the upper mantle essentially invariant. We shall return to this point below.

2. For the crustal velocity cross-section we have assumed, we are unable to resolve the uppermost 20 km or so of the mantle just below the Moho. This is illustrated by solutions 47, 45, 46, 53 in Fig. 3. These four acceptable models have the same values of crustal thickness (55 km), lid thickness (20 km), channel thickness (110 km) and channel velocity (4.33 km/sec); the four models differ only by virtue of their lid velocities which range from 4.21 to 4.51 km/sec. Our conclusion is that a thin veneer of material of either high or low S-wave velocity located just beneath the Moho cannot be detected by our methods, and such a thin layer may or may not be present. As will be shown below, our preferred models are those with low-velocity material at the top of the mantle; in this case, a thin veneer of low-velocity material is not significant since it blends with the rest of the mantle. Thus, we state that we are unable to tell if a thin veneer of high-velocity material is present or not.

3. Because of our inability to detect thin veneers, we focus our attention now on solutions with lid thickness 30 km or greater. In Fig. 4 we show the values of upper mantle velocities that have been found to be acceptable within the criterion of fit by at least one structure. The circled entries give the number of solutions with these values of velocity. The fact that there are more solutions in one part of model space than in another is not persuasive. If the data are valid, the "real earth" can lie anywhere within the triangular region of Fig. 4, including the *unpopular* parts of this region.

A number of models have lid velocities of 4.31 or 4.41 km/sec; these values are unusually low for normal stable continental regions (Biswas and Knopoff, 1974 (4); Knopoff, 1972) (13). The low upper mantle velocities represented by the cases of $\beta_{LID} = 4.31$ or 4.41 km/sec extend to depths which we cannot determine adequately with these data; we can accommodate positive and negative gradients of velocity as well as solutions with substantially no gradient, but in any case all these models have unusually low S-wave velocities immediately below the Moho.

Structures with *S*-wave velocities of the order of 4.3 km/sec immediately below the Moho have been obtained in inversion of phase velocities measured across the Colorado Plateau (Biswas and Knopoff, 1974) (4). The phase velocity for a two-station profile from Golden, Colorado to Dugway, Utah is reproduced in Fig. 2 for comparison.

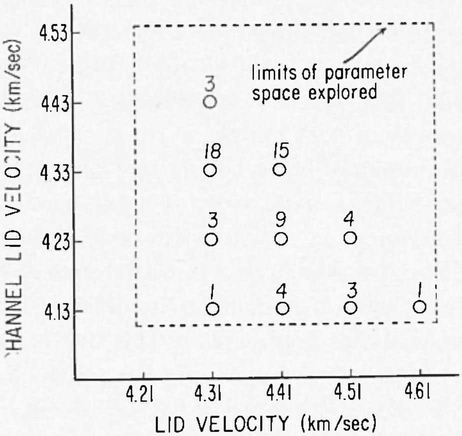

Fig. 4 – Two-dimensional shear-wave velocity space of acceptable solutions obtained from Hedgehog inversion with lid thickness greater than or equal to 30 km.

Except at the shortest periods, the phase velocities for TNO-AQU and GOL-DUG are remarkably similar. Thus, it is reasonable that the inversions for these two regions give similar results; the differences at short periods can be attributed to differences in crustal structure.

The solutions with lid velocity 4.51 km/sec (Nos. 20, 24, 21, 39, 29, 27, 23) or 4.61 km/sec (No. 50) present a different kind of picture. In these cases, we have a lid of thickness up to 40 km below the Moho overlying a channel of velocity from 4.13 to 4.23 km/sec. (We did not seek solutions with channel velocities lower than 4.13 km/sec.) In these cases, we have a relatively high velocity lid overlying a channel with remarkably low *S*-wave velocities. Channel velocities this low have been observed in the oceans (Berry and Knopoff, 1967 (3); Leeds et al., 1974) (17) and in the Alps (Knopoff et al., 1966) (14). In the latter case, upper mantle models SPLA-(C,N) have crustal thicknesses of 40 or 50 km, lids extending to depths of about 80 km, lid velocities of 4.5 km/sec or so, and channel velocities of 4.15 km/sec or so; these models are very similar to model 29 in Fig. 3. One important difference between the Alpine models and this subset of Apennines models is the differing thickness of low-velocity channel; we believe that we cannot resolve the bottom of the channel with either set of data in view of the limited period range.

In Fig. 2, we have also plotted the phase velocity for an Alpine profile extending from Besançon to Chur (event 6 October, 1960) reported by Knopoff et al. (1966) [14] which led to the Alpine models under comparison. The phase velocities for BES-CHU differ from TNO-AQU by more than 0.05 km/sec at about 40 sec and perhaps also at 80 sec. The discrepancy between the two phase velocities at 40 sec illustrates the need for a good crustal structure: we attribute this discrepancy to differences in crustal structure; certainly our model of a uniform crust for the Apennines is too simple. The difference in phase velocities at 80 sec, if real, must be attributed to differences in channel thickness, with the Alpine channel extending to greater depths.

4. How can we resolve the differences between the two groups of models, namely, those with relatively low upper mantle velocities ($V_s \sim 4.3$ km/sec) starting at the Moho and extending downward (the Colorado Plateau model) and the model with a thin lid of high velocities overlying a channel with exceptionally low velocities ($V_s \sim 4.15$ km/sec) (the Alpine model)? In our view, the resolution will come only when more adequate information about the crustal structure can be obtained. Caloi (1957), [8] using earthquake travel-times, has indicated that the Appennines in this region have a crustal thickness of about 45 km. While this result is close to our value and may be correct, the paucity of data used in the study indicates that one should place greater emphasis on results obtained by refraction methods. Much to the south of the regions under consideration here, Colombi et al. (1973) [9] have found a crustal thickness of the order of 40 to 45 km under the Apennines by refraction methods. Based on sketchy information, Giese and Morelli (1973) [10] have attributed a crustal thickness to this region of 25 to 30 km, a figure in marked contrast to our value. Giese and Morelli also indicate that the preferred *Pn* velocity in this region is about 7.2 km/sec These values indicate the presence of extraordinarily low-velocity material just below the Moho, since a decrease in crustal thickness, as has already been noted, accompanies a decrease in mantle lid velocity. We believe that our value of crustal thickness

may be a consequence of our oversimplified crustal model. This would then indicate a preference for our models of Colorado Plateau type over the Alpine type.

Some support for this point of view should be found in geothermal evidence. If the mantle-lid *S*-wave velocities are low, starting from the Moho and extending downward, high surface heat flow should be observed. There is certainly geothermal activity in this area; a heat flow measurement at Larderello by Boldiszar (1963) (5) is 6 to 14 HFU. Larderello is hardly a typical location, but the presence of significant hot spring activity is important information that cannot be ignored.

Conclusions

Rayleigh wave phase-velocity observations over the path TNO-AQU indicate that there is a significant amount of low-velocity material in the mantle under the Apennines. The indications of low *P*-wave velocities at shallow depth, plus hot spring activity, when coupled with the inversion of our surface-wave observations, support the notion that low-velocity material in the mantle is found within a few km of the Moho and may lie immediately below the Moho; we cannot completely reject an alternative model, namely, that there is a high-velocity lid of thickness 30 to 40 km overlying a very low-velocity channel with *S*-wave velocities in the channel of about 4.1 to 4.2 km/sec.

Unfortunately, our observations are for earthquakes lying on only one side of the station pair TNO-AQU. A *reversed profile*, in which we observe dispersion for surface waves arriving at the same stations from the south, is much to be hoped for since this would test the reality of attributing our observations to the structure between the two stations.

Acknowledgments

The authors wish to acknowledge the assistance of M. Gasperini (Bologna), W. Mitronovas (Zurich), J. Schlue (Los Angeles) and D. Seidl (Karlsrühe) for installation and maintenance of the long-period network. This work was supported by grants from the Consiglio Nazionale delle Ricerche, the Deutsche Forschungsgemeinschaft and N.A.T.O.

REFERENCES

(1) BACKUS, G. and F. GILBERT, 1968. – *The resolving power of gross earth data*, "Geophys. J. Roy. Astron. Soc.", **16**, pp. 169-205.

(2) BACKUS, G. and F. GILBERT, 1970. – *Uniqueness in the inversion of inaccurate gross earth data.* "Phil. Trans. R. Soc. Lond.", **266A**, pp. 123-192.

(3) BERRY, M. J., and L. KNOPOFF, 1967. – *Structure of the upper mantle under the Western Mediterranean Basin*, "J. Geophys. Res.", **72**, pp. 3613-3626.

(4) BISWAS, N. N., and L. KNOPOFF, 1974. – *Structure of the upper mantle underthe United States fromt he dispersion of Rayleigh waves.* "Geophys. J. Roy. Astron. Soc.", **36**, pp. 515-539.

(5) BOLDIZSAR, T., 1963. – *Terrestrial heat flow in the natural stream field at Larderello.* "Geofis. Pura Appl.", **56**, pp. 115-122.

(6) BOLT, B. A., and J. DORMAN, 1961. – *Phase and group velocities of Rayleigh waves in a spherical, gravitating earth*, "J. Geophys. Res.", pp. **66**, 2965-2981.

(7) BRUNE, J., and J. DORMAN, 1963. – *Seismic waves and earth structures in the Canadian shield*, "Bull. Seismol. Soc. Amer.", **53**, pp. 167-210.

(8) CALOI, P., 1957. – *Caratteristiche della crosta terrestre dalle Alpi agli Appennini*, "Annali di Geofisica", **10**, pp. 189-192.

(9) COLOMBI, B., P. GIESE, G. LUONGO, C. MORELLI, M. RIUSCETTI, S. SCARASCIA, K. G. SCHUTTE, J. STROWALD and G. DE VISINTINI, 1973. – *Preliminary report on the seismic refraction profile Gargano-Salerno-Palermo-Pantelleria (1971).* "Boll. Geofis. Teor. ed Appl.", **15**, pp. 225-254.

(10) GIESE, P., and C. MORELLI, 1973. – *Structural map of the "Moho".* In "Structural Model of Italy", Sheet South 2, CNR, Rome.

(11) JACKSON, D. D., 1972. – *Interpretation of inaccurate, insufficient and inconsistent data.* "Geophys. J. Roy. Astron. Soc.", **28**, pp. 97-109.

(12) JAMES, D. E., 1971. – *Andean crustal and upper mantle structure.* "J. Geophys. Res.", **76**, pp. 3246-3271.

(13) KNOPOFF, L., 1972. – *Observation and inversion of surface wave dispersion.* "Tectonophysics", **13**, pp. 497-519.

(14) KNOPOFF, L., St. MUELLER and W. L. PILANT, 1966. – *Structure of the crust and upper mantle in the Alps from the phase velocity of Rayleigh waves.* "Bull. Seismol. Soc. Amer", **56**, pp. 1009-1044.

(15) KNOPOFF, L., and J. W. SCHLUE, 1972. – *Rayleigh wave phase velocities for the path Addis Ababa-Nairobi.* "Tectonophysics", **15**, pp. 157-163.

(16) LEEDS, A. R., 1975 – *Lithospheric thickness in the Western Pacific.* "Phys. Earth & Planet. Interiors", **11**, p. 61-64.

(17) LEEDS, A. R., L. KNOPOFF and E. G. KAUSEL, 1974. – *Variations of upper mantle structure under the Pacific Ocean.* "Science", **186**, pp. 139-141.

(18) PANZA, G. F., 1976. – *Phase velocity determination of fundamental Love and Rayleigh waves.* "Pure Appl. Geophys.", **114**, pp. 753-763.

(19) PILANT, W. L., and L. KNOPOFF, 1964. – *Observation of multiple seismic events.* "Bull. Seismol. Soc. Amer.", **54**, pp. 19-39.

(20) SEIDL, D., H. REICHENBACH and St. MUELLER, 1970. – *Dispersion investigations of Rayleigh waves in the Rhinegraben rift system.* In "Graben Problems", pp. 203-206 J. H. Illies and St. Mueller, eds. (Schweizerbart Verlag, Stuttgart, 1970).